PHYSICAL REVIEW LETTERS

ॐ

# Remote Preparation of an Atomic Quantum Memory

Wenjamin Rosenfeld,[1,*] Stefan Berner,[1] Jürgen Volz,[1] Markus Weber,[1] and Harald Weinfurter[1,2]

[1]*Department für Physik, Ludwig-Maximilians Universität München, D-80799 München, Germany*
[2]*Max-Planck Institut für Quantenoptik, D-85748 Garching, Germany*
(Received 14 August 2006; published 2 February 2007)

Storage and distribution of quantum information are key elements of quantum information processing and future quantum communication networks. Here, using atom-photon entanglement as the main physical resource, we experimentally demonstrate the preparation of a distant atomic quantum memory. Applying a quantum teleportation protocol on a locally prepared state of a photonic qubit, we realized this so-called remote state preparation on a single, optically trapped $^{87}$Rb atom. We evaluated the performance of this scheme by the full tomography of the prepared atomic state, reaching an average fidelity of 82%.

Quantum information science has already shown many new possibilities for information processing and communication, most prominently, secure communication [1] and the efficient solution of certain computational problems which cannot be efficiently treated on a classical computer [2]. For future applications, such as links between quantum computers or long distance quantum communication, new devices are required. While photons are ideal for the transfer of qubits (as the generalization of the classical bit the basic entity of quantum information), matter carriers of the qubits, e.g., atoms, ions, superconducting circuits, or quantum dots are well suited for storage and processing. Many new concepts, for example, the quantum repeater [3] or quantum networks for distributed quantum computing thus require the faithful mapping of quantum information between photonic quantum channels and matter-based quantum memories and processors. Entanglement between matter and light is crucial for achieving this task.

So far, there are two methods experimentally investigated. The first employs atomic ensembles of about $10^6$–$10^{12}$ atoms to momentarily store quantum states of light. Recently, qubits encoded on single photons or qunits encoded in the quantum state of an electromagnetic field have been transferred to the collective state of atoms and vice versa [4,5]. An impressive experimental demonstration of a first quantum communication protocol, the quantum teleportation of coherent states of light onto an atomic ensemble, was reported very recently [6].

The second method is based on the recently achieved entanglement between a single atom and a single photon [7,8]. It applies directly to well-studied single quantum systems like trapped neutral atoms or ions, where various methods of quantum information storage and processing were already demonstrated, e.g., entanglement of up to 8 ions [9,10], creation of a cluster state involving tens of neutral atoms [11], or manipulations on a neutral atom quantum shift register [12]. Furthermore, this interface concept can be adopted to other qubit systems, like optically addressed quantum dots [13–15] or superconducting QED systems [16], stimulating novel applications in these areas as well.

Here we experimentally prove the suitability of atom-photon entanglement as the interface between a memory device and the quantum communication channel. For this purpose we perform the full remote preparation of an atomic quantum memory via teleportation of an arbitrarily prepared quantum state of a single photon.

Similar to quantum teleportation [17], remote state preparation (RSP) [18,19] starts with entanglement between two quantum systems (in our case atom-photon). Whereas in quantum teleportation the qubit to be transferred is carried by a third particle, in RSP it is encoded in an additional degree of freedom of the particle given to the sender, usually called Alice. The other one of the two particles of the entangled pair is sent to the receiver, called Bob, and will carry the qubit after the successful termination of the protocol. This consists of two steps, first, a complete Bell-state measurement between the qubit encoding the quantum state to be sent and the entangled qubit of the sender. Second, the result obtained in this measurement (2 bits of classical information) is communicated to the receiver. He uses this information to perform one out of four well-defined, state independent transformations, thereby reconstructing or preparing the original state. Recently, various approaches towards remote state preparation were studied experimentally with entangled photons [20], light beams [21], and nuclear magnetic spins [22]. However without expansion of the Hilbert space, and thus without the possibility of complete Bell-state analysis, such experiments are limited to a maximum efficiency of 50% and/or are introducing state dependency of the method.

To demonstrate the full RSP protocol, our experiment includes four steps: (i) Entanglement is generated between the spin of a single trapped $^{87}$Rb atom and the polarization of a single spontaneously emitted photon [8]. (ii) An additional degree of freedom of the photon is used to encode the quantum state we wish to transfer [18]. (iii) The photon is subject to a complete Bell-state measurement [19,23], projecting the atom into one of four well-defined states. (iv) The success of the transfer is shown with full quantum state tomography of the atomic qubit.

In more detail, we first establish entanglement between a photon and a single neutral $^{87}$Rb atom stored in an optical dipole trap [24]. Therefore the atom is optically excited to the $5^2P_{3/2}$, $|F' = 0, m_{F'} = 0\rangle$ state [see Fig. 1(a)]. In the following spontaneous decay the polarization of the emitted photon is entangled with the spin state of the atom [8], resulting in the maximally entangled state

$$|\Psi^+\rangle = \frac{1}{\sqrt{2}}(|\downarrow\rangle_z|\sigma^+\rangle + |\uparrow\rangle_z|\sigma^-\rangle), \qquad (1)$$

where $|\sigma^\pm\rangle$ are the right- and left-circular polarization states of the emitted photon. The two states $|\uparrow\rangle_z$ and $|\downarrow\rangle_z$, defining the atomic qubit, correspond to the $|F = 1, m_F = \pm 1\rangle$ Zeeman sublevels of the $5^2S_{1/2}$, $F = 1$ hyperfine ground level.

For the next step, the emitted photon is coupled into a single-mode optical fiber [Fig. 1(b)] and guided to the setup shown in Fig. 2, where the state we wish to transfer is imprinted onto the photon. For this purpose we extend the Hilbert space of the photon by using two spatial modes as an additional degree of freedom. The photon is coherently split into the two spatial modes $|a\rangle$ and $|b\rangle$ by means of a polarization independent Mach-Zehnder interferometer, resulting in the spatial state $\cos(\frac{\alpha}{2})|a\rangle + \sin(\frac{\alpha}{2})|b\rangle$. The phase $\alpha$ is determined by the optical path-length difference between the two interferometer arms. Next, the two spatial modes acquire an additional phase difference $\phi$, resulting in the state

$$e^{i\phi} \cos\left(\frac{\alpha}{2}\right)|a\rangle + \sin\left(\frac{\alpha}{2}\right)|b\rangle \qquad (2)$$

of the photonic qubit. In order to prepare a well-defined state, precise control over the interferometric phases $(\alpha, \phi)$ is necessary. Therefore the optical path-length differences in the interferometric setup are actively stabilized with the help of an additional stabilization laser and an electronic feedback loop, allowing measurement times of up to 24 h. By inserting a rotatable glass plate into the stabilization beam we can change these path-length differences and thus precisely control the phase setting.
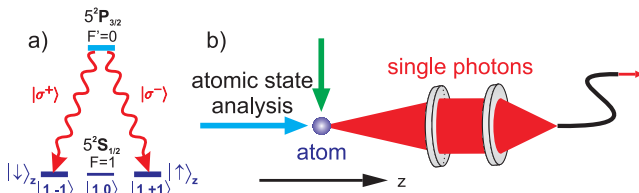


FIG. 1 (color online). Schematic of atom-photon entanglement generation in a spontaneous decay of a single optically trapped $^{87}$Rb atom. (a) After optical excitation to $F' = 0$, the atom decays into the ground state manifold $|\uparrow\rangle_z$, $|\downarrow\rangle_z$ forming an entangled state between the atomic spin and the polarization of the emitted photon. (b) The emitted photon is collected with a microscope objective, coupled into a 5 m long single-mode optical fiber and guided to the preparation setup shown in Fig. 2. The overall detection efficiency for the photon is about $3 \times 10^{-4}$.

Next, to transfer the state given by Eq. (2) onto the spin state of the atom, a Bell-state measurement in the joint polarization–spatial-mode Hilbert space of the photon is performed. This is done by combining the two modes $|a\rangle$ and $|b\rangle$ on a polarizing beam splitter (PBS) and analyzing the photon polarization in each output port (see Fig. 2). The polarization analyzer detects $|\pm 45°\rangle = \frac{1}{\sqrt{2}}(|H\rangle \pm |V\rangle)$ polarized photons by means of four single photon counting Si avalanche photo diodes (APD1-4). Since the PBS transmits horizontal $|H\rangle$ and reflects vertical $|V\rangle$ polarization, a coherent superposition of orthogonal polarizations from both modes is necessary to obtain $|\pm 45°\rangle$ in the output of the PBS. For example, to get $|+45°\rangle$ in the PBS output with detectors 1 and 2, $|H\rangle$ polarization has to be transmitted from mode $|b\rangle$ and coherently added to $|V\rangle$ polarization reflected from mode $|a\rangle$. This corresponds to the Bell state $|\Psi^+\rangle = \frac{1}{\sqrt{2}}(|V\rangle|a\rangle + |H\rangle|b\rangle)$. Accordingly, the $|-45°\rangle$ polarization corresponds to the $|\Psi^-\rangle = \frac{1}{\sqrt{2}} \times (|V\rangle|a\rangle - |H\rangle|b\rangle)$ state, while in the other output of the PBS the states $|\Phi^\pm\rangle = \frac{1}{\sqrt{2}}(|H\rangle|a\rangle \pm |V\rangle|b\rangle)$ are detected.

The Bell-state detection projects the atomic qubit onto one of the four states

$$|\Phi_1\rangle = e^{i\phi} \cos\left(\frac{\alpha}{2}\right)|\uparrow\rangle_x + \sin\left(\frac{\alpha}{2}\right)|\downarrow\rangle_x,$$

$$|\Phi_2\rangle = e^{i\phi} \cos\left(\frac{\alpha}{2}\right)|\uparrow\rangle_x - \sin\left(\frac{\alpha}{2}\right)|\downarrow\rangle_x,$$

$$|\Phi_3\rangle = e^{i\phi} \cos\left(\frac{\alpha}{2}\right)|\downarrow\rangle_x - \sin\left(\frac{\alpha}{2}\right)|\uparrow\rangle_x, \qquad (3)$$

$$|\Phi_4\rangle = e^{i\phi} \cos\left(\frac{\alpha}{2}\right)|\downarrow\rangle_x + \sin\left(\frac{\alpha}{2}\right)|\uparrow\rangle_x,$$
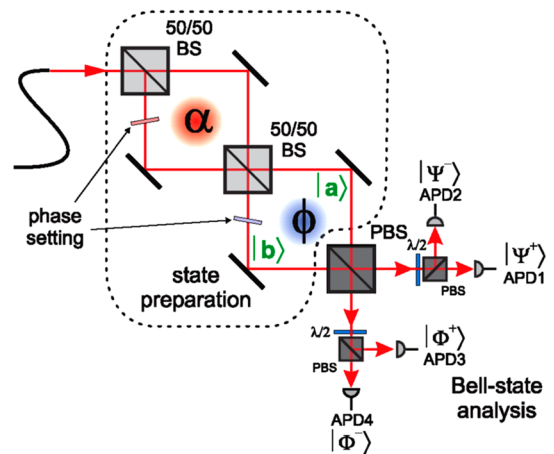


FIG. 2 (color online). Schematic setup for preparing the state from Eq. (2) on the spatial degree of freedom of the photon and for the subsequent Bell-state measurement. The interferometric phase setting $(\alpha, \phi)$ allows to prepare any desired superposition of the spatial modes $|a\rangle$ and $|b\rangle$ without affecting the polarization degree of freedom. The following PBS, together with the polarization measurement in $|\pm45°\rangle$, basis enable a complete Bell-state analysis in the combined polarization–spatial-mode Hilbert space of the photon.

where $|\uparrow\rangle_x$, $|\downarrow\rangle_x = \frac{1}{\sqrt{2}}(|\uparrow\rangle_z \pm |\downarrow\rangle_z)$. State $|\Phi_1\rangle$ is already equivalent to the photonic state from Eq. (2). The states $|\Phi_2\rangle$, $|\Phi_3\rangle$, and $|\Phi_4\rangle$ can be transformed into $|\Phi_1\rangle$ by applying the operation $\hat{\sigma}_x$, $\hat{\sigma}_y$, or $\hat{\sigma}_z$, respectively, on the atom.

After completion of the transfer of the state from the photon to the atom we perform the analysis of the atomic state [8]. First, a certain superposition of $|\uparrow\rangle_z$ and $|\downarrow\rangle_z$ is transferred to the $5^2S_{1/2}$, $F = 2$ hyperfine ground level by means of a state-selective STIRAP process. The polarization of the transfer pulse defines which superposition is transferred and thus allows the choice of the measurement basis. The following hyperfine-state analysis measures the fraction of population which was transferred from the $|F = 1\rangle$ to the $|F = 2\rangle$ ground level. This method allows to analyze the state of the atom in any desired basis and thus to reconstruct the density matrix of the state by combining measurements in 3 complementary bases. The characterization of the entangled atom-photon state with this method yields a fidelity of 87%.

In order to evaluate the performance of our preparation scheme, we prepared different states of the atom by varying the phase settings ($\alpha$, $\phi$). Then we performed a full quantum state tomography of the atomic qubit for each of the four detected Bell states separately. Figure 3 exemplarily shows a measurement where we set $\alpha = 90°$ while rotating $\phi$ from 0° to 330° in steps of 30°. Let us consider, e.g., the state which is prepared when the photon is registered in detector APD1. This state can be decomposed as

$$|\Phi_1\rangle = \cos\left(\frac{1}{2}\left(\phi + \frac{\pi}{2}\right)\right)|\uparrow\rangle_z + i\sin\left(\frac{1}{2}\left(\phi + \frac{\pi}{2}\right)\right)|\downarrow\rangle_z$$
$$= \frac{1}{\sqrt{2}}(e^{i\phi}|\uparrow\rangle_x + |\downarrow\rangle_x) = \cos\left(\frac{1}{2}\phi\right)|\uparrow\rangle_y + i\sin\left(\frac{1}{2}\phi\right)|\downarrow\rangle_y.$$

(4)

While the projections of $|\Phi_1\rangle$ onto $|\uparrow\rangle_x$ and $|\downarrow\rangle_x$ are equal and constant, we observe a dependence on $\phi$ for the projection onto $|\uparrow\rangle_z$, $|\downarrow\rangle_z$, and $|\uparrow\rangle_y$, $|\downarrow\rangle_y$. By combining all three measurements we determined the density matrix of each prepared atomic state. From this we derived the fidelity [which is the probability to find the atom in the state expected from Eq. (3)] for each detector and every setting of ($\alpha$, $\phi$). The mean fidelity over all points and all four analyzed Bell states in this measurement is 82.6%. We performed 4 sets of measurements of this kind preparing various states on different circles on the Bloch sphere (see Fig. 4). Altogether, 42 different states were prepared with a mean fidelity of 82.2% (see Table I).

There are several sources of imperfections which affect the achieved preparation fidelity. The most important factors are the limited purity of the generated entangled atom-photon state and imperfections in the atomic state detection, yielding together a reduced entanglement fidelity of 87%. Taking into account this error source we get a corrected fidelity of $\frac{0.82}{0.87} \approx 94\%$ for the preparation and
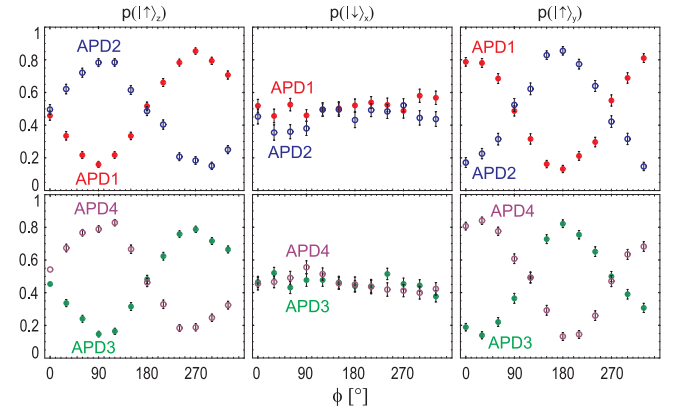


FIG. 3 (color online). Tomographic data set of the prepared atomic states for $\alpha = 90°$, $\phi = 0–330°$. The figures show the probability $p$ to find the atom in the state $|\uparrow\rangle_z$ (left), $|\downarrow\rangle_x = \frac{1}{\sqrt{2}} \times (|\uparrow\rangle_z - |\downarrow\rangle_z)$ (middle), and $|\uparrow\rangle_y = \frac{1}{\sqrt{2}}(|\uparrow\rangle_z + i|\downarrow\rangle_z)$ (right), respectively, after a photon detection in detector 1 (red, filled) and 2 (blue, hollow) (upper row), 3 (green, filled) and 4 (magenta, hollow) (lower row). Each data point is evaluated from 150–350 measurement processes from which we calculate the depicted statistical errors (1 standard deviation). The mean fidelity of the 12 states prepared in this measurement is 82.6%. The acquisition of the full data set was realized within approximately three days at an event rate of 10–20 per min.

teleportation process alone. This value is limited by the finite visibility of the interferometer and Bell-state analyzer (about 96%), the mechanical instability of the interferometer and the residual birefringence of its components. The coherence of the prepared states decays on a time scale of about 10 $\mu$s and does not influence the current measurement. This decay is caused solely by dephasing due to magnetic stray fields, resulting from instabilities of the magnetic environment. Longer coherence times will be achieved by using an improved compensation method.

The principles enabling the successful remote state preparation now also can be applied to further quantum communication protocols, e.g., the quantum repeater. High-$Q$ cavities can enhance the emission probability of the photon into a particular mode, and thus also the rates, by more than 2 orders of magnitude [25]. These cavities should host several atoms [12], which are first entangled with atoms in one of two neighboring cavities via individual entanglement swapping [26]. Second, the entanglement of the atoms with the ones in the other cavities is purified in order to correct for noise and imperfections. One thereby obtains two entangled atoms in each cavity (except for the outermost ones), where always one of them is highly entangled with one in the two neighboring cavities. A Bell-state measurement on such two atoms swaps the entanglement to the atoms in the neighboring cavities. After similar sequences of purification and entanglement swapping over longer and longer links one finally obtains entanglement between the outermost atoms of this chain. Because of the event-ready signal from the entanglement
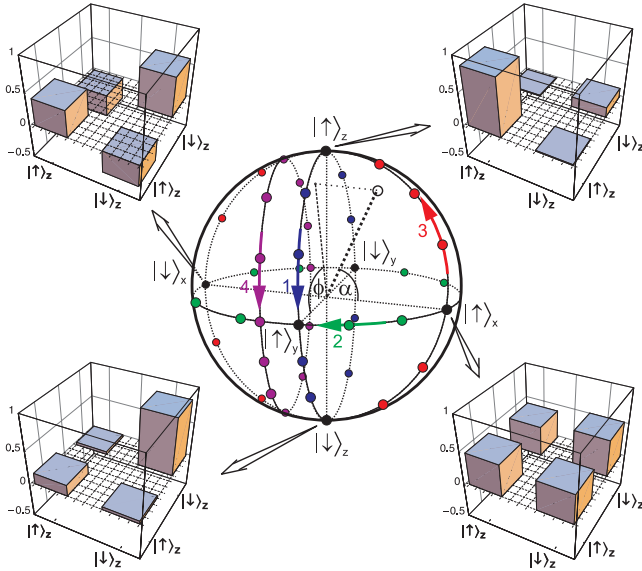
FIG. 4 (color online).    Bloch-sphere representation of the states prepared on the atomic qubit. The basis states in the equatorial plane are defined as $|\uparrow\rangle_x$, $|\downarrow\rangle_x := \frac{1}{\sqrt{2}}(|\uparrow\rangle_z \pm |\downarrow\rangle_z)$ and $|\uparrow\rangle_y$, $|\downarrow\rangle_y := \frac{1}{\sqrt{2}}(|\uparrow\rangle_z \pm i|\downarrow\rangle_z)$. The angles $(\alpha, \phi)$ can be interpreted as usual polar coordinates with respect to the $x$ axis. The numbers 1–4 depict the corresponding measurements from Table I. The insets exemplarily show measured density matrices of the atomic qubit (real part) for four selected states.

swapping to the atoms, the number of steps scales polynomially and enables efficient long distance communication [3]. This way one profits from both the high fidelity and flexibility of quantum logic operations on atoms or ions and the efficient transmission of photonic qubits that are ideally suited for long distance distribution of quantum information.

In conclusion, the presented experiment demonstrates the faithful remote preparation of arbitrary quantum states of a single atom without the need of a direct interaction between the information carrier (photon) and the quantum memory (atom). Our implementation uses a quantum teleportation protocol to transfer the state of a photonic qubit onto the atom with an average preparation fidelity as high

as 82%. Together with the long coherence time of atomic ground states [27] such a system is well suited for future applications and makes the quantum repeater—almost—state of the art.

*Corresponding author.
Electronic address: Wenjamin.Rosenfeld@physik.uni-muenchen.de

[1] N. Gisin, G. Ribordy, W. Tittel, and H. Zbinden, Rev. Mod. Phys. **74**, 145 (2002).
[2] M. A. Nielsen and I. L. Chuang, *Quantum Computation and Quantum Information* (Cambridge University Press, Cambridge, England, 2000).
[3] H.-J. Briegel, W. Dür, J. I. Cirac, and P. Zoller, Phys. Rev. Lett. **81**, 5932 (1998).
[4] D. Matsukevich and A. Kuzmich, Science **306**, 663 (2004).
[5] B. Julsgaard *et al.*, Nature (London) **432**, 482 (2004).
[6] J. Sherson *et al.*, Nature (London) **443**, 557 (2006).
[7] B. B. Blinov, D. L. Moehring, L. M. Duan, and C. Monroe, Nature (London) **428**, 153 (2004).
[8] J. Volz *et al.*, Phys. Rev. Lett. **96**, 030404 (2006).
[9] H. Häffner *et al.*, Nature (London) **438**, 643 (2005).
[10] D. Leibfried *et al.*, Nature (London) **438**, 639 (2005).
[11] O. Mandel *et al.*, Nature (London) **425**, 937 (2003).
[12] Y. Miroshnychenko *et al.*, Nature (London) **442**, 151 (2006).
[13] X. Li *et al.*, Science **301**, 809 (2003).
[14] A. Badolato *et al.*, Science **308**, 1158 (2005).
[15] L. Childress *et al.*, Phys. Rev. Lett. **96**, 070504 (2006).
[16] A. Wallraff *et al.*, Nature (London) **431**, 162 (2004).
[17] C. H. Bennett *et al.*, Phys. Rev. Lett. **70**, 1895 (1993); D. Bouwmeester *et al.*, Nature (London) **390**, 575 (1997); A. Furusawa *et al.*, Science **282**, 706 (1998); I. Marcikic *et al.*, Nature (London) **421**, 509 (2003); M. Riebe *et al.*, Nature (London) **429**, 734 (2004); M. D. Barrett *et al.*, Nature (London) **429**, 737 (2004).
[18] S. Popescu, quant-ph/9501020.
[19] D. Boschi *et al.*, Phys. Rev. Lett. **80**, 1121 (1998).
[20] N. Peters *et al.*, Phys. Rev. Lett. **94**, 150502 (2005).
[21] S. A. Babichev, B. Brezger, and A. I. Lvovsky, Phys. Rev. Lett. **92**, 047903 (2004).
[22] X. Peng *et al.*, Phys. Lett. A **306**, 271 (2003).
[23] M. Michler, Ph.D. thesis, University of Vienna, 2000.
[24] M. Weber, J. Volz, K. Saucke, C. Kurtsiefer, and H. Weinfurter, Phys. Rev. A **73**, 043406 (2006).
[25] T. Wilk, S. C. Webster, H. P. Specht, G. Rempe, and A. Kuhn, quant-ph/0610227.
[26] M. Zukowski *et al.*, Phys. Rev. Lett. **71**, 4287 (1993); J.-W. Pan *et al.*, Phys. Rev. Lett. **80**, 3891 (1998).
[27] R. A. Cline, J. D. Miller, M. R. Matthews, and D. J. Heinzen, Opt. Lett. **19**, 207 (1994).

TABLE I.    Summary of the experimental results. The table shows the fidelity $F$, i.e., the probability of a successful state transfer for different phase settings $(\alpha, \phi)$, averaged over the 4 detected Bell states and all 12 points within one measurement set.

| # | $\alpha$ | $\phi$ | $F$ |
|---|---|---|---|
| 1 | 90° | 0° – 330° | 82.6% ± 0.40% |
| 2 | 0° – 330° | 0° | 79.7% ± 0.65% |
| 3 | 0° – 330° | 90° | 84.2% ± 0.45% |
| 4 | 109.5° | 0° – 330° | 82.2% ± 0.46% |